doi:10.1038/nature10758

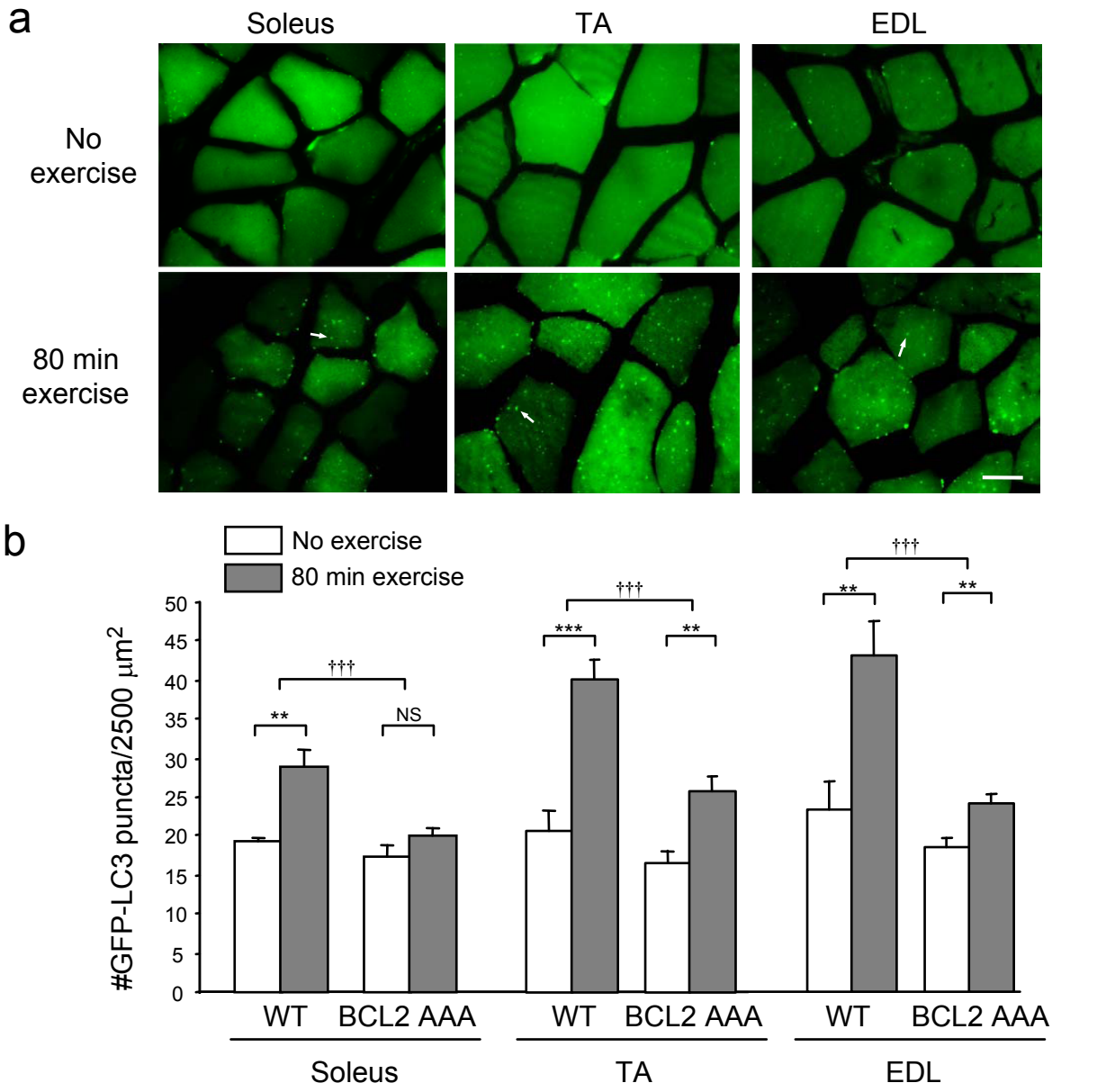

Supplementary Figure 1. Exercise induces BCL2-regulated autophagy in different muscle groups. a, Representative images of GFP-LC3 puncta (autophagosomes) in indicated muscle groups of GFP-LC3 WT transgenic mice at baseline and after 80 min of exercise. Arrows denote representative autophagosomes. Scale bar, 20 µm. **b,** Quantification of GFP-LC3 puncta in indicated muscle groups of GFP-LC3 WT and GFP-LC3 BCL2 AAA mice before and after 80 min of exercise. A minimum of 10 fields per mouse was analyzed. Results represent mean ± s.d. for 3 mice per experimental group. TA, tibialis anterior; EDL, extensor digitorum longus. $^{**}P < 0.01$, $^{***}P < 0.001$, one-way ANOVA for comparison between groups; †††$P < 0.001$, two-way ANOVA for comparison of magnitude of changes between different groups in mice of different genotypes. NS, not significant.

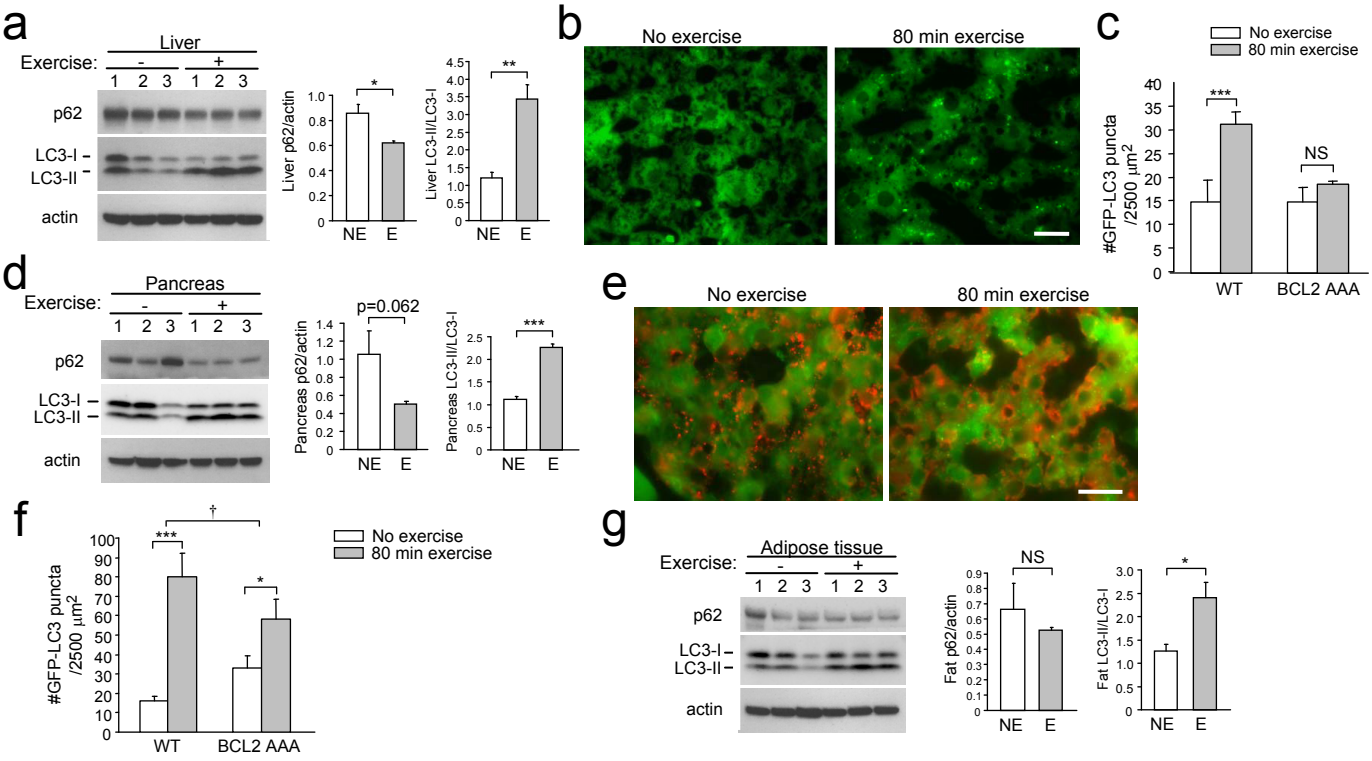

Supplementary Figure 2. Exercise induces BCL2-regulated autophagy in liver, and pancreas. a, Biochemical analysis of autophagy induction in livers from WT mice at rest (-) or after maximal exercise by Western blot detection of p62 and LC3-II conversion (left). Actin is shown as a loading control. Graphs showing quantification of p62/actin and LC3-II/LC3-I ratios at rest (NE) and after exercise (E) for 3 mice per group (right). Results represent mean ± s.e.m. **b,** Representative images of GFP-LC3 puncta (autophagosomes) in hepatocytes from GFP-LC3 WT mice at rest and after 80 min of exercise. **c,** Quantification of the number of GFP-LC3 puncta in hepatocytes from WT and BCL2 AAA mice at rest and after 80 min of exercise. GFP-LC3 puncta increase with exercise in WT but not in BCL2 AAA mice. **d,** Biochemical analysis of autophagy induction in pancreas from WT mice at rest (-) or after maximal exercise by Western blot detection of p62 and LC3-II conversion (left). Actin is shown as a loading control. Graphs showing quantification of p62/actin and LC3-II/LC3-I ratios at rest (NE) and after exercise (E) for 3 mice per group (right). Results represent mean ± s.e.m. **e,** Representative images of GFP-LC3 puncta in pancreatic β-cells from GFP-LC3 WT mice at rest and after 80 min of exercise. Pancreatic sections were immunostained with an anti-insulin antibody to label β-cells (red color). **f,** Quantification of the number of GFP-LC3 puncta in pancreatic β-cells from WT and BCL2 AAA mice at rest and after 80 min of exercise. GFP-LC3 puncta increase with exercise in both WT mice and BCL2 AAA mice; the magnitude of increase with exercise is greater in WT mice. For (**c**) and (**f**), results represent mean ± s.d. for 3 mice per experimental group. A minimum of 10 fields was analyzed per mouse. **g,** Biochemical analysis of autophagy induction in adipose tissue from WT mice at rest (-) or after maximal exercise by Western blot detection of p62 and LC3-II conversion (left). Actin is shown as a loading control. Graphs showing quantification of p62/actin and LC3-II/LC3-I ratios at rest (NE) and after exercise (E) for 3 mice per group (right). Results represent mean ± s.e.m. Scale bar, 20 μm. $*P < 0.05$, $**P < 0.01$, $***P < 0.001$, one-way ANOVA for comparison between groups; $\dagger P < 0.05$, two-way ANOVA for comparison of magnitude of changes between different groups in mice of different genotypes. NS, not significant.

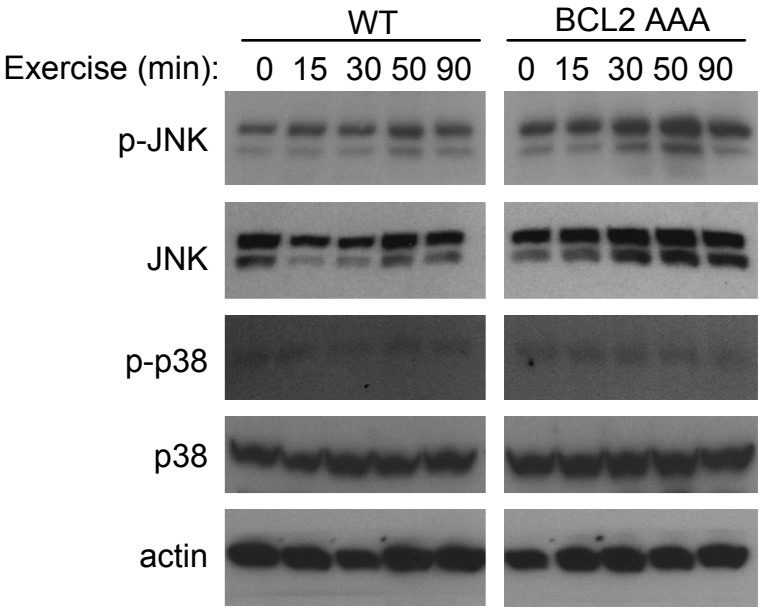

Supplementary Figure 3. Absence of exercise-induced activation of MAPK signaling in muscle. Western blot analysis of phosphorylated and total levels of JNK and p38 at indicated time points after exercise in vastus lateralis muscle of WT and BCL2 AAA mice. Actin is shown as a loading control. p-JNK, phospho-JNK; p-p38, phospho-p38.

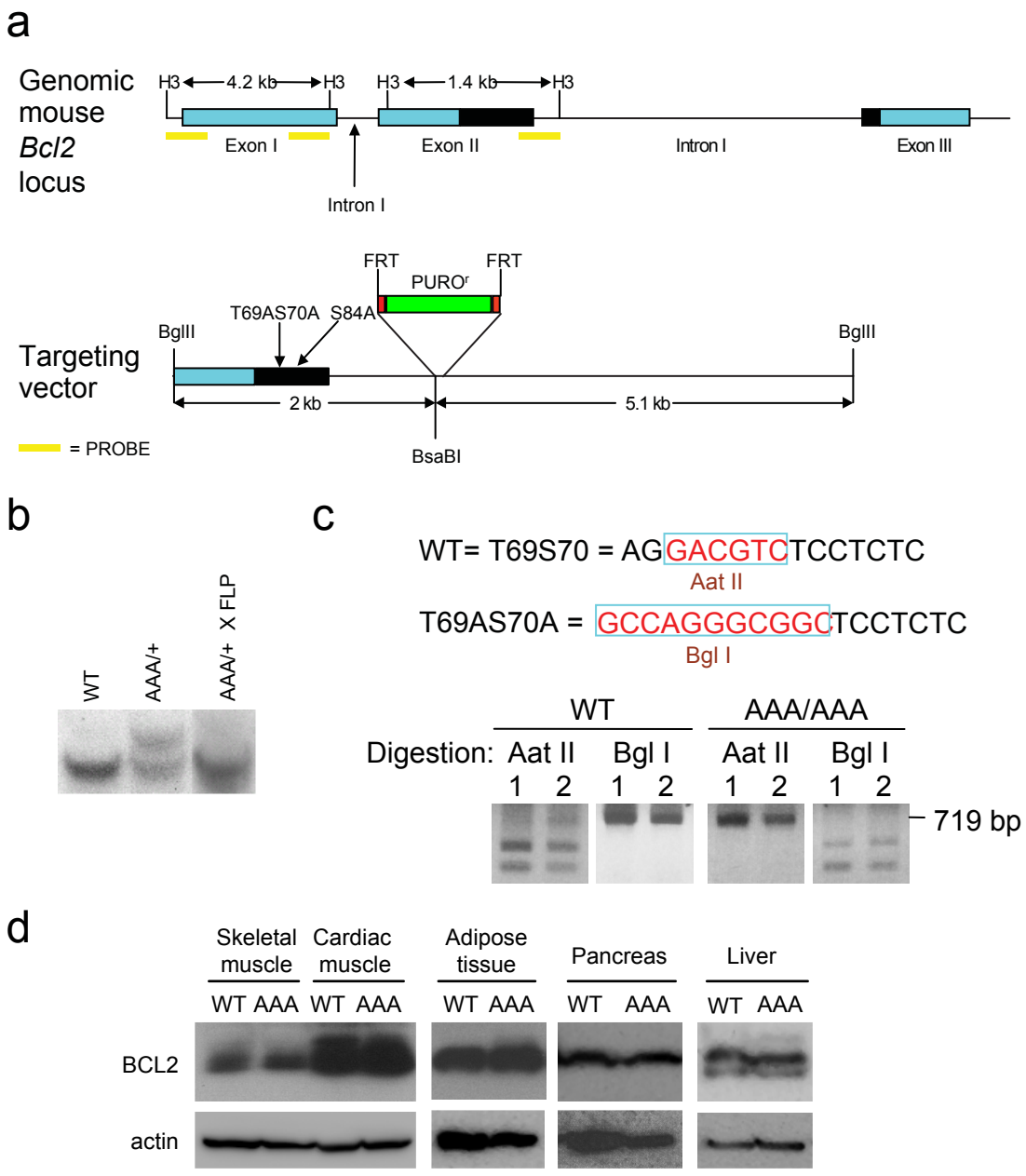

Supplementary Figure 4. Generation of BCL2 AAA knock-in mice. a, Genomic structure of *Bcl2* and the *Bcl2*^{AAA} knock-in vector. The coding region in exon II was targeted with the 5' arm of the targeting vector. A short PstI fragment containing the loop region was excised, mutated to a nucleotide sequence encoding amino acids T69A, S70A, S84A, and replaced. FRT sites allowed for excision of the puromycin resistance marker upon breeding to FLP mice. **b,** Targeting of the *Bcl2* locus identified by a 1.7 kb upshift in the locus by Southern blot. Excision of the puromycin marker returned the digested fragment to WT size following breeding to FLP mice. **c,** Mutant sites identified by restriction digestion of the 719 bp PCR-amplified coding fragment. **d,** Western blot analysis of protein extracts from skeletal and cardiac muscle, adipose tissue, liver, and pancreas of *Bcl2*^{WT} (WT) and *Bcl2*^{AAA} (BCL2 AAA) mice to detect levels of mouse BCL2 expression. Actin is shown as a loading control.

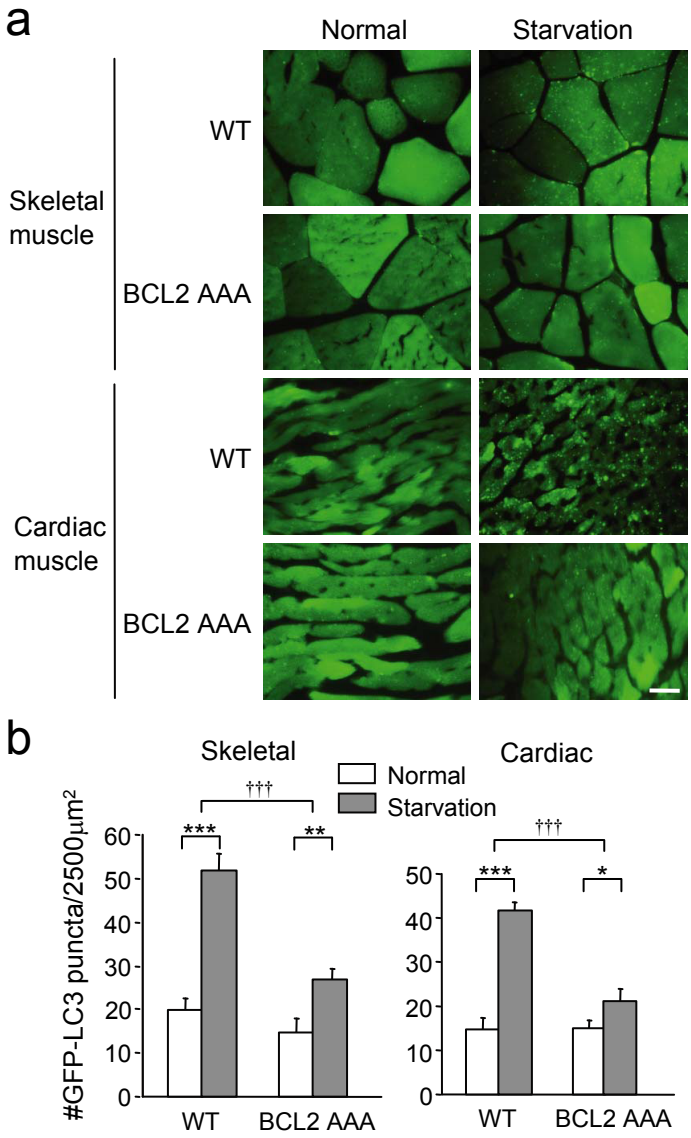

Supplementary Figure 5. Defects in starvation-induced autophagy in skeletal and cardiac muscle of BCL2 AAA mice. a, Representave images of GFP-LC3 puncta (autophagosomes) in skeletal (vastus lateralis) and cardiac muscle of GFP-LC3 WT and GFP-LC3 BCL2 AAA mice that were either fed a normal diet or starved for 48 h. Scale bar, 20 μm. **b,** Quantification of the GFP-LC3 puncta shown in (**a**). Results represent mean ± s.d. of 4 mice per experimental group. **P* < 0.05, ***P* < 0.01, ****P* < 0.001, one-way ANOVA for comparison between groups; †††*P* < 0.001, two-way ANOVA for comparison of magnitude of changes between different groups in mice of different genotypes.

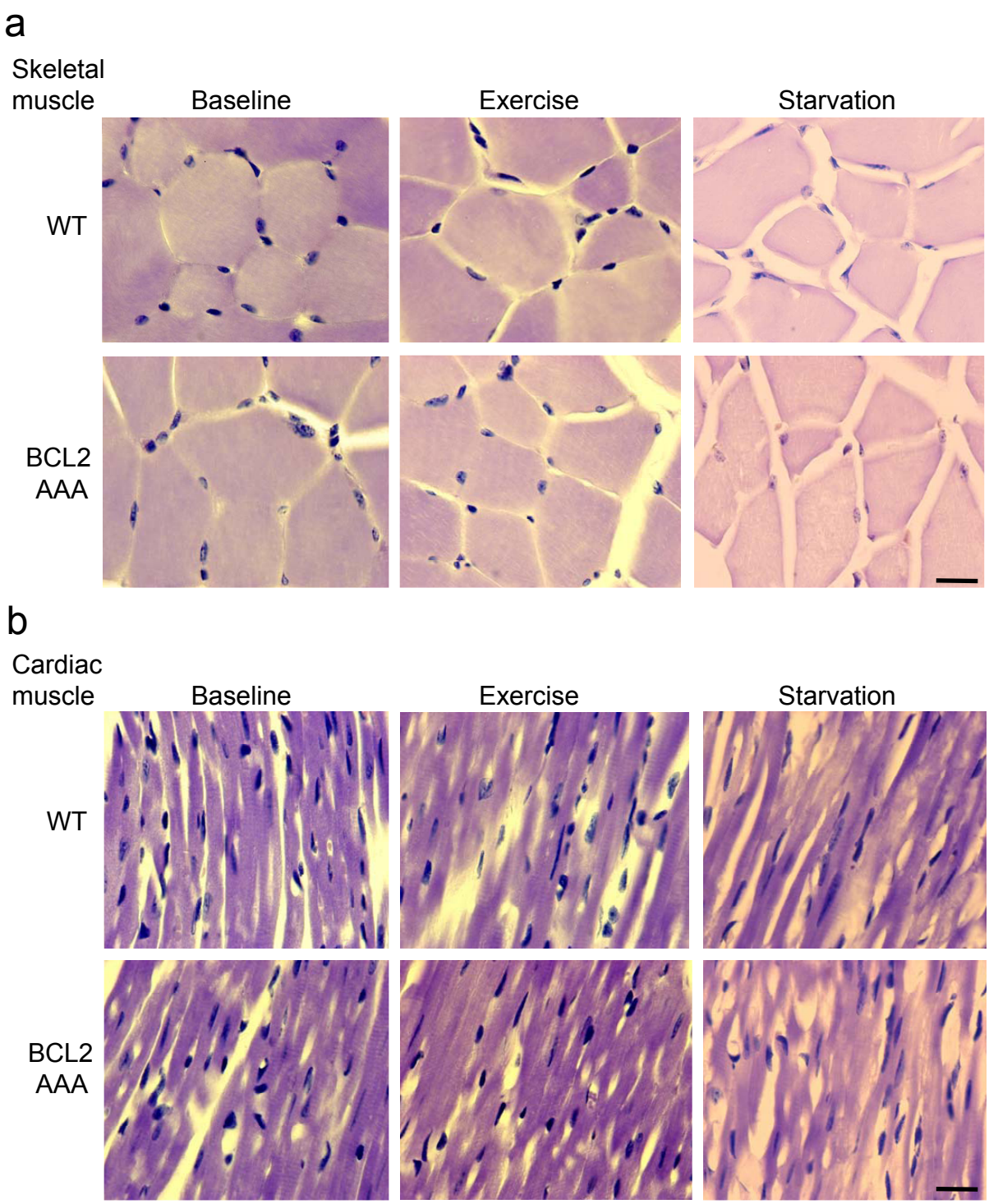

Supplementary Figure 6. Absence of apoptosis in skeletal and cardiac muscle in response to starvation or exercise. Representative images of TUNEL staining to detect apoptotic cells in skeletal (vastus lateralis) muscle (**a**) or cardiac muscle (**b**) of WT and BCL2 AAA mice at baseline, after 48 h of starvation, or after 80 min of exercise. Mouse tissue samples with TUNEL-positive cells from laboratory reference slides were used as a positive control for TUNEL staining (not shown). Three mice per genotype were examined per experimental condition. Scale bar, 20 μm.

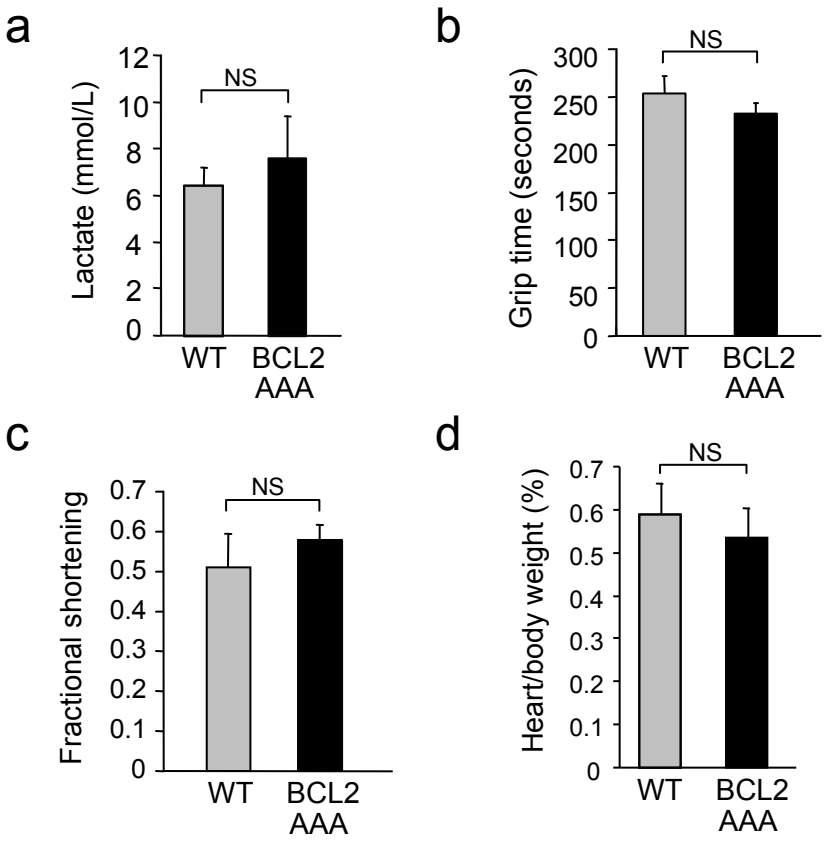

Supplementary Figure 7. BCL2 AAA and WT mice have similar exercise-induced lactate production, muscle grip strength, and cardiac function and weight. a, Plasma lactate levels in WT and BCL2 AAA mice after maximal exercise. Results represent mean ± s.e.m. of 4-6 mice per experimental group. **b,** Muscle strength of WT and BCL2 AAA mice as measured by grip time on a wire mesh. Results represent mean ± s.e.m. of 6 mice per experimental group. **c,** Cardiac function of WT and BCL2 AAA mice as determined by echocardiographic measurement of fractional shortening. Results represent mean ± s.e.m. of 3 mice per experimental group. **d,** Cardiac weight of WT and BCL2 AAA mice calculated as a percentage of total body weight. Results represent mean ± s.d. cardiac weight for 5 mice per group. NS, not significant (one-way ANOVA).

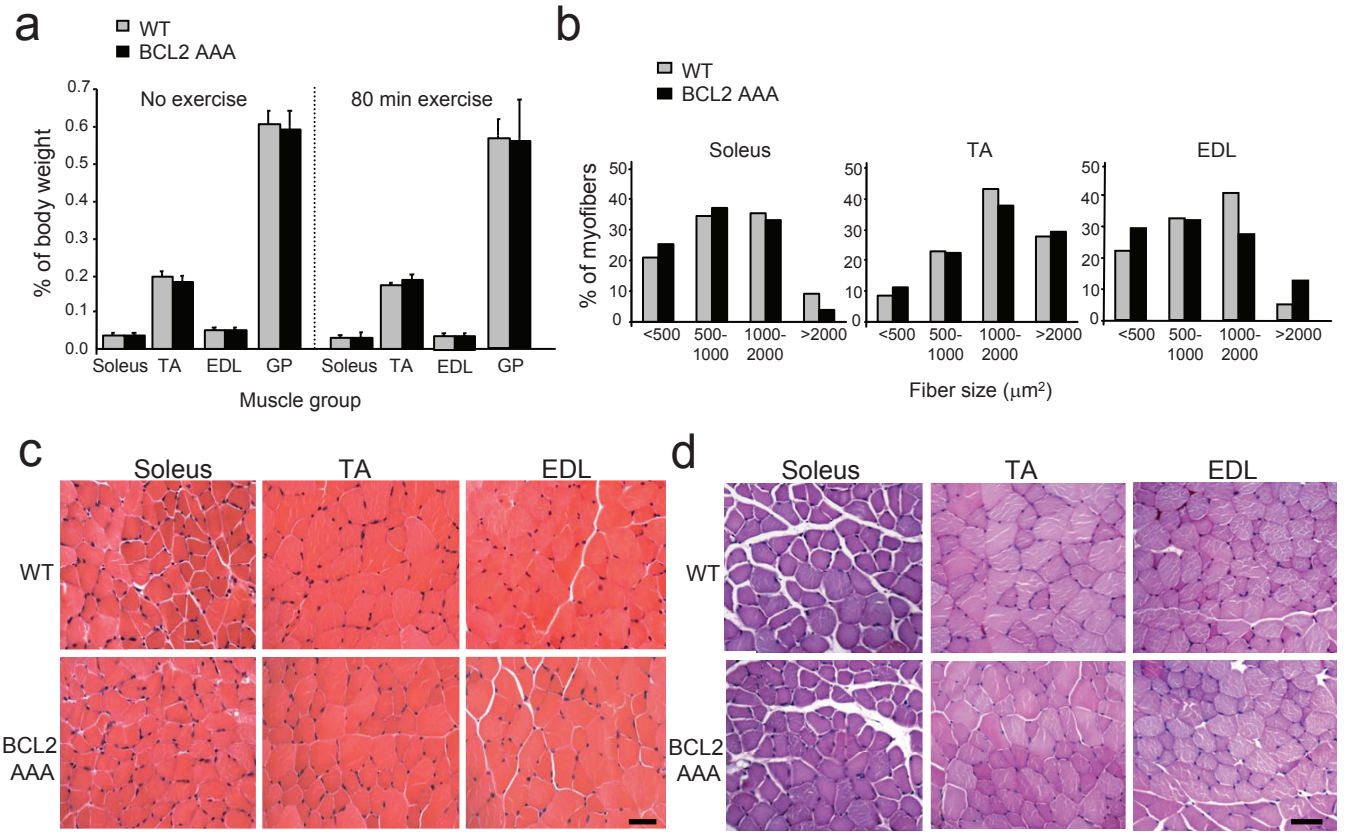

Supplementary Figure 8. BCL2 AAA and WT mice have similar muscle morphology. a, Different muscle groups from WT or BCL2 AAA mice at baseline or after 80 min of treadmill exercise were dissected and weighed. Muscle weight was calculated as percentage of total body weight. Results represent mean ± s.d. of 6 mice per experimental group. **b,** Muscle fiber cross sectional area in different muscle groups of WT or BCL2 AAA mice was measured using laminin staining to outline each fiber. Myofibers from 3 muscle cross-sections per mouse of 3 mice per genotype were measured. Approximately 600 myofibers were measured for the soleus and EDL muscle groups and approximately 1000 myofibers were measured for the TA muscle group. Results represent combined data for 3 mice per muscle group per genotype and are expressed as the percentage of myofibers within each category of cross-sectional area. **c,** H&E staining of indicated muscle groups from WT and BCL2 AAA mice. Similar results were observed in 3 mice per genotype. **d,** Periodic acid-Schiff (PAS) staining of indicated muscle groups of WT and BCL2 AAA mice. Similar results were observed in 3 mice per genotype For **b-d**, experiments were performed at baseline conditions (without exercise). TA, tibialis anterior; EDL, extensor digitorum longus; GP, gastrocnemius-plantaris. Scale bar, 40 μm.

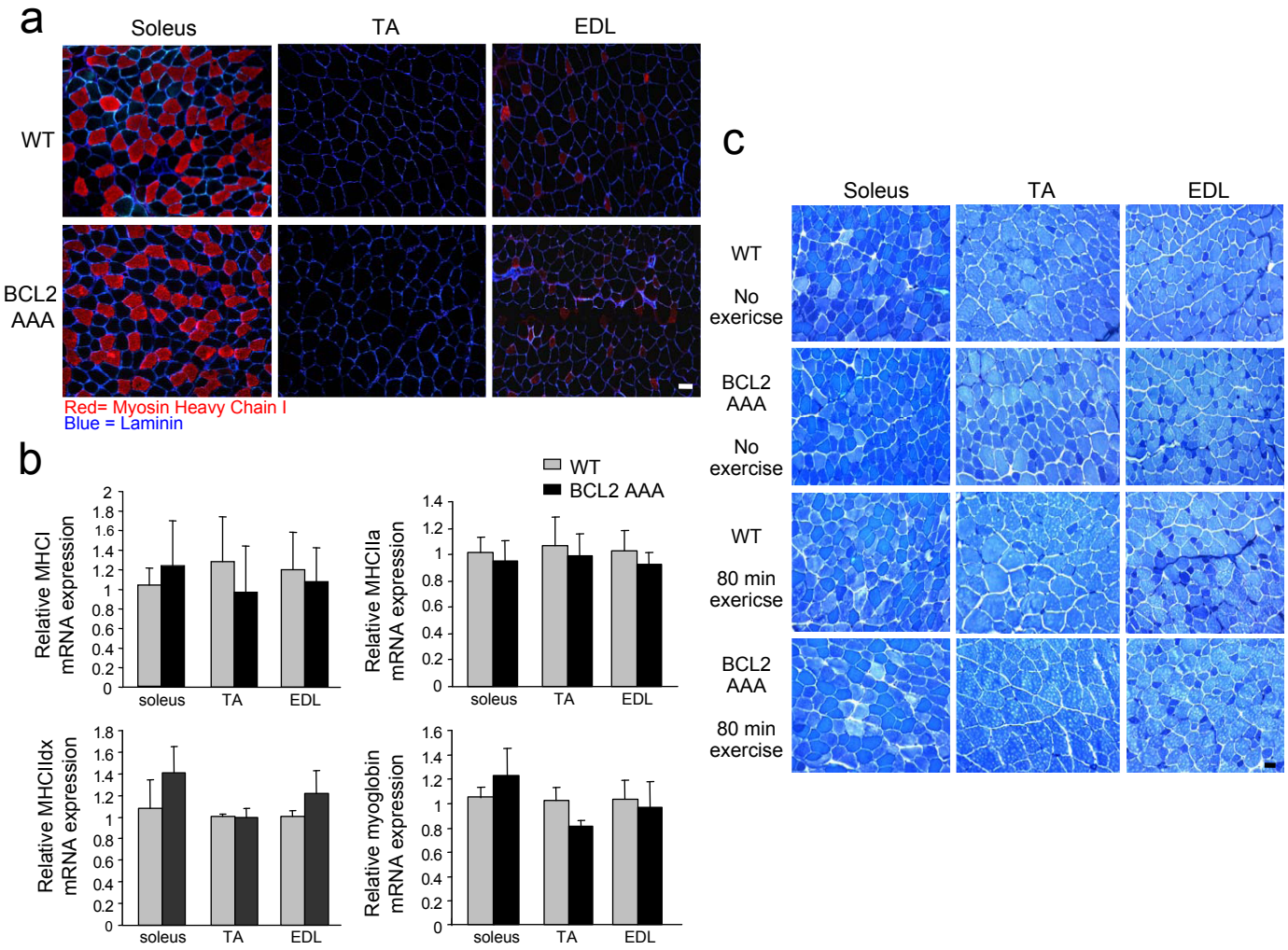

Supplementary Figure 9. Absence of detectable differences in fiber type analyses of various muscle groups from WT and BCL2 AAA mice. a, Immunostaining of MHCI (myosin heavy chain I) (red color) and laminin to outline myofibers (blue color) of indicated muscle groups from WT and BCL2 AAA mice. Similar results were observed in 3 mice per genotype per muscle group. **b,** Real-time RT-PCR analysis of the expression of indicated muscle fiber type marker in indicated muscle groups from WT and BCL2 AAA mice. For each marker, data for each muscle group from BCL2 AAA mice were normalized to levels of corresponding muscle group in WT mice. Results represent mean ± s.e.m of 4 mice per experimental group. No statistically significant differences were observed for relative expression of any of the fiber type markers in any muscle group between WT and BCL2 AAA mice (ANOVA). **c,** Metachromatic staining of ATPase activity in different muscle groups of WT and BCL2 AAA mice during baseline conditions and after 80 min of exercise. TA, tibialis anterior; EDL, extensor digitorum longus. Scale bar, 40 μm.

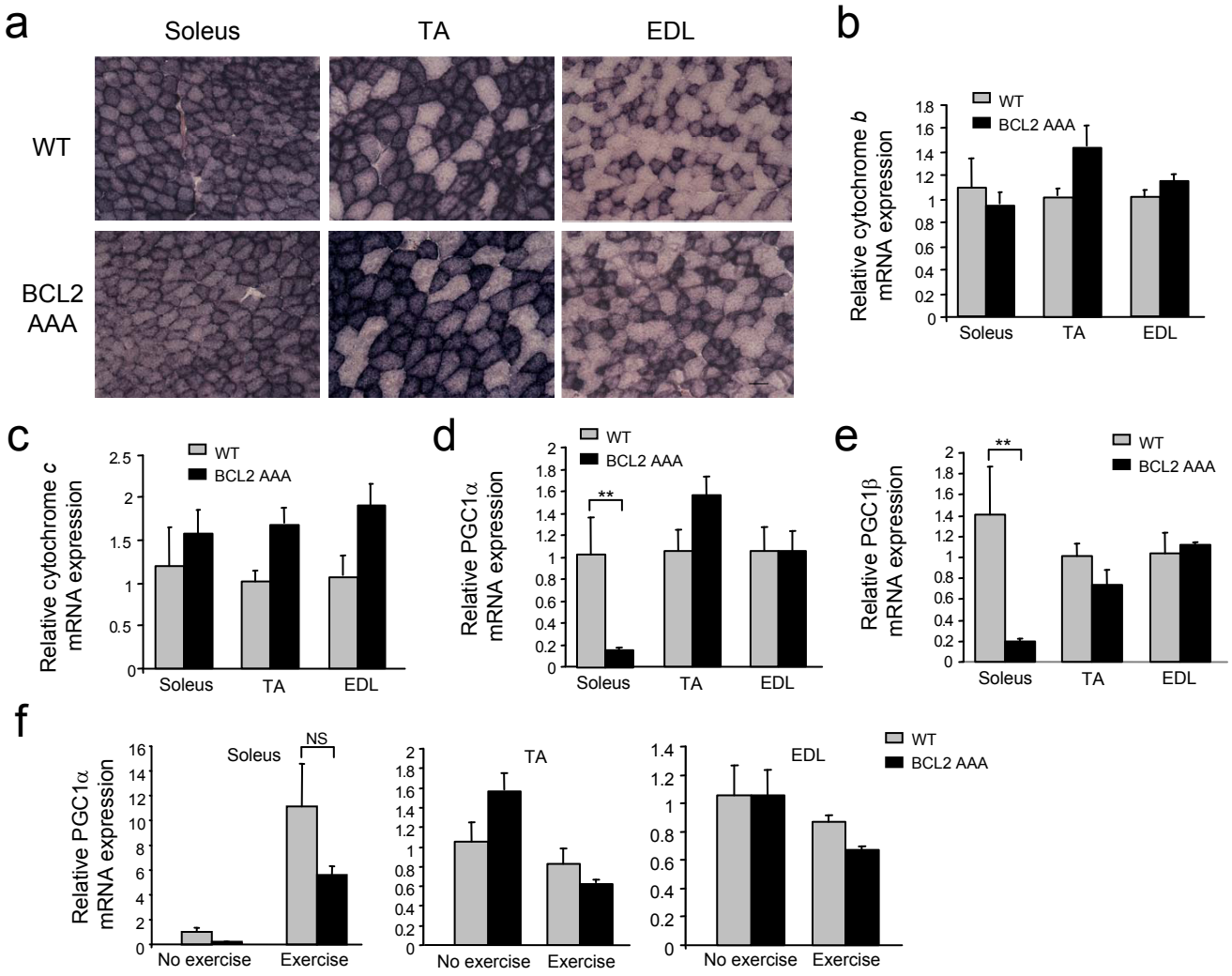

Supplementary Figure 10. Mitochondrial content and function is not significantly altered in muscle groups of BCL2 AAA vs. WT mice. a, Detection of mitochondrial SDH (succinate dehydrogenase) activity (dark purple color) of indicated muscle groups from WT and BCL2 AAA mice. **b-e**, Real-time RT-PCR analysis of various mitochondrial markers in indicated muscle groups of WT and BCL2 AAA mice during baseline conditions to detect relative mRNA expression of cytochrome *b* (**b**), cytochrome *c* (**c**), PGC1α (**d**) and PGC1β (**e**). For each marker, data for each muscle group from BCL2 AAA mice were normalized to levels of corresponding muscle group in WT mice. **f,** Real-time RT-PCR analysis of PGC1α expression in indicated muscle groups of WT and BCL2 AAA mice during baseline conditions or after 80 min of exercise. Data for each muscle group in each genotype were normalized to levels of expression in WT mice during resting conditions. For **b-f**, results represent mean ± s.e.m of 4 mice per experimental group. For **b-f**, the only statistically significant differences between WT and BCL2 AAA mice for each marker in each muscle type were for PGC1α and PGC1β mRNA expression in the soleus muscle during resting conditions. No significant differences were observed in PGC1α expression levels in exercised BCL2 AAA compared to WT mice but the magnitude of PGC1α induction with exercise was greater in BCL2 AAA compared to WT mice ($P < 0.05$, 2-way ANOVA). TA, tibialis anterior; EDL, extensor digitorum longus. $^{**}P < 0.01$ (one-way ANOVA). NS, not significant.

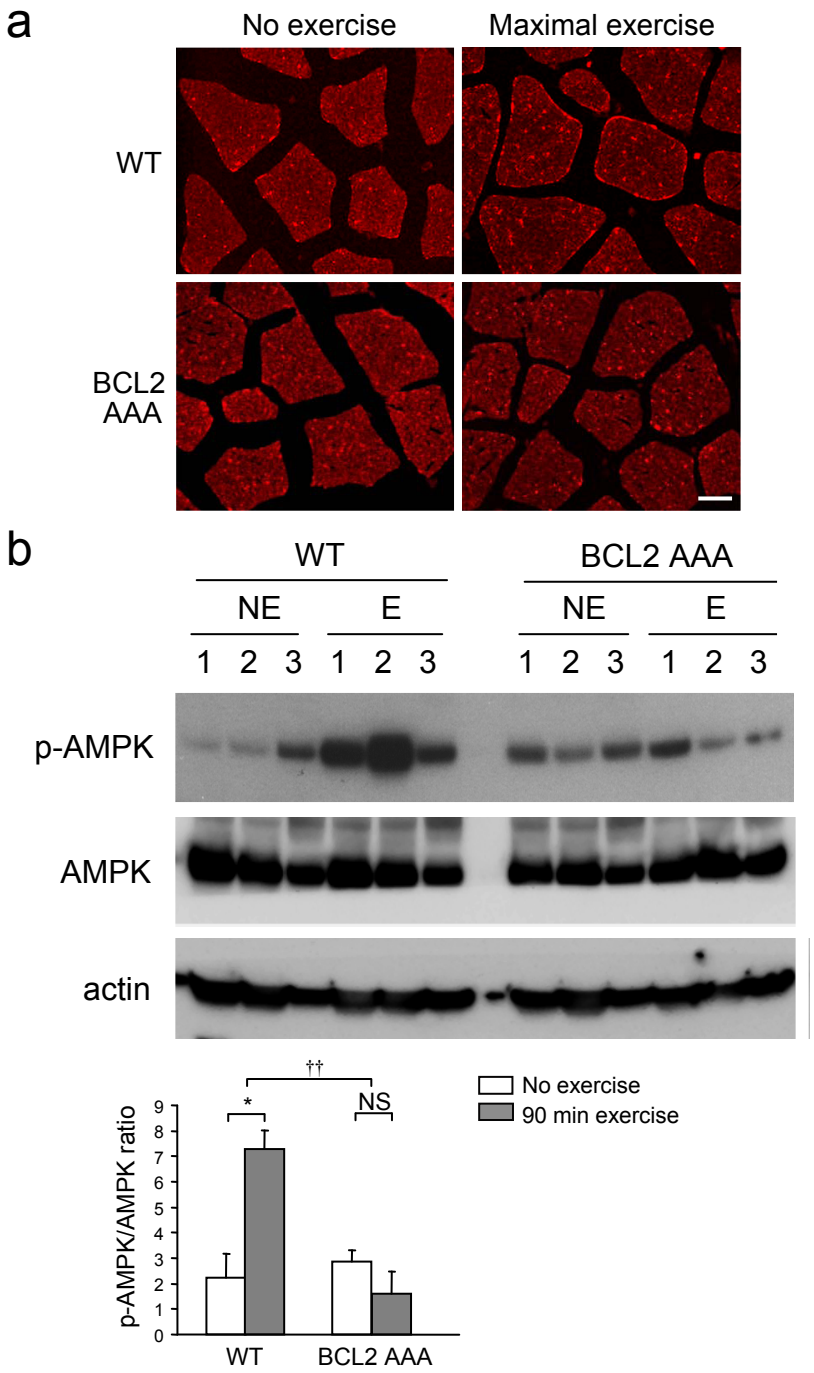

Supplementary Figure 11. Deficient exercise-induced GLUT4 translocation and AMPK activation in muscle of BCL2 AAA mice. a, Representative confocal immunofluorescence images showing subcellular localization pattern of GLUT4 in the vastus lateralis muscle of WT and BCL2 AAA mice before and after maximal exercise. Scale bar, 20 μm. **b,** Western blot analysis of phosphorylated and total levels of AMPK at resting conditions or after 90 min of exercise in vastus lateralis muscle of WT and BCL2 AAA mice. Three mice per experimental group are shown. Actin is shown as a loading control. Graph below shows quantification of p-AMPK/AMPK ratio at rest (no exercise) and after 90 min of exercise. Results represent mean ± s.e.m. *$P < 0.05$, one-way ANOVA for comparison between groups; ††$P < 0.01$, two-way ANOVA for comparison of magnitude of changes between different groups in mice of different genotypes. NS, not significant.

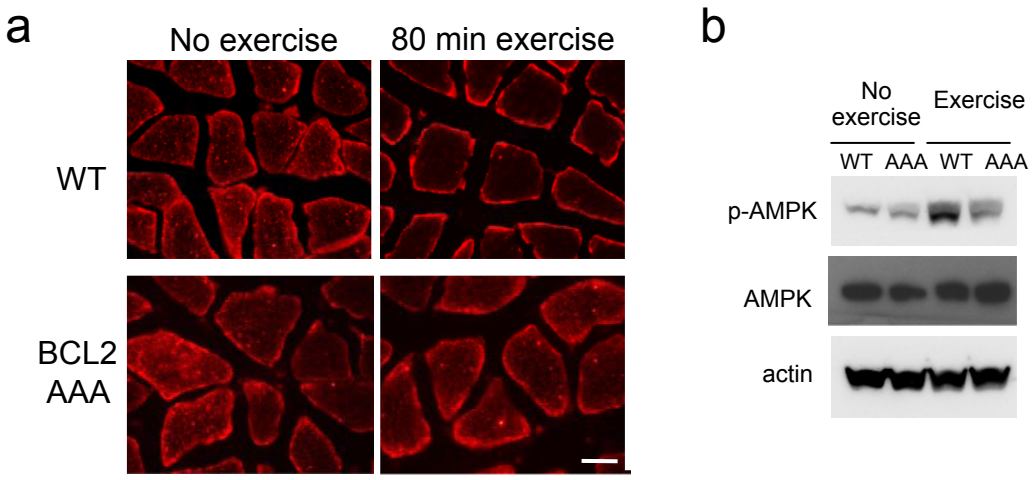

Supplementary Figure 12. Exercise-induced GLUT4 plasma membrane translocation and AMPK activation is deficient in the soleus muscle of BCL2 AAA mice. a, Representative immunofluorescence images demonstrating subcellular localization pattern of GLUT4 in the soleus muscle of WT and BCL2 AAA mice during baseline conditions and after 80 min of exercise. Scale bar, 20 μm. Similar results were observed in 3 mice per group. **b,** Levels of AMPK phosphorylation in soleus muscle lysates from WT and BCL2 AAA mice during baseline conditions and after 80 min of exercise. Similar results were observed in 3 mice per genotype per experimental condition.

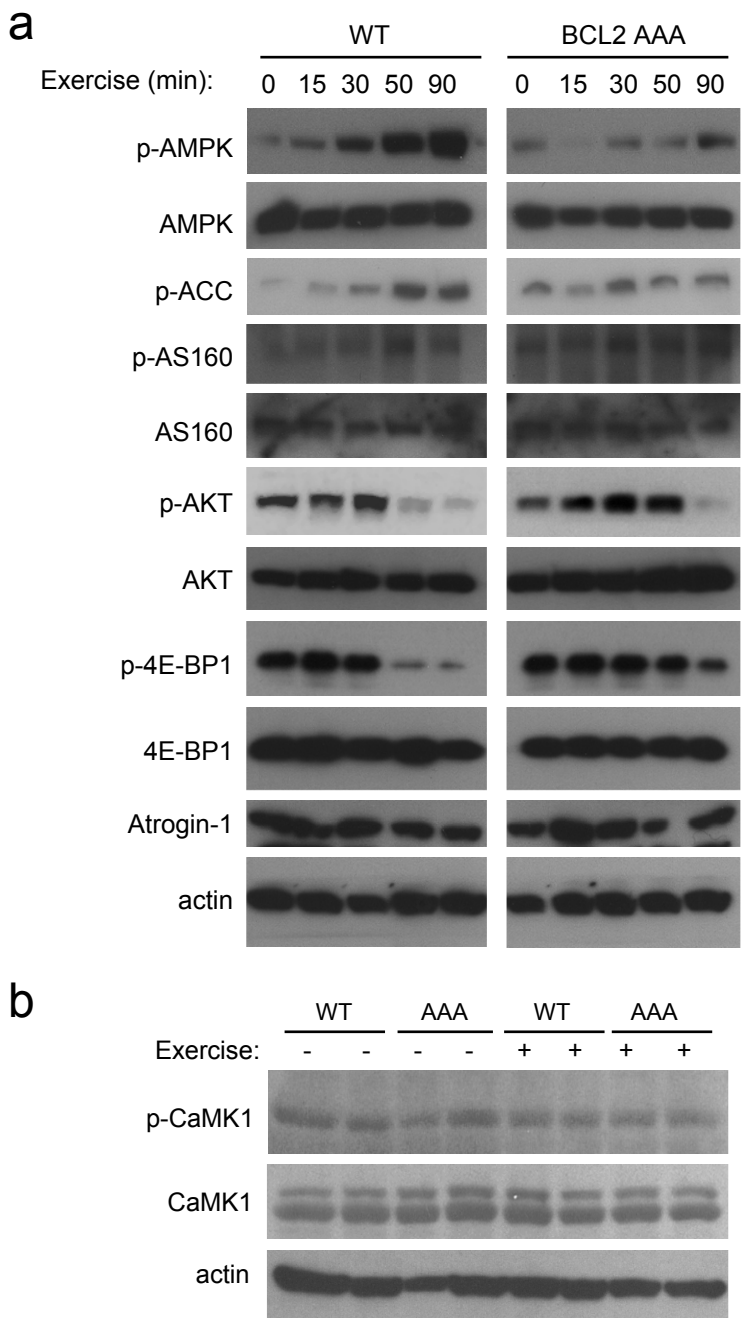

Supplementary Figure 13. Analysis of the AMPK, AKT, mTOR, FoxO and CaMK1 signaling pathways in muscle after exercise in WT and BCL2 AAA mice. a, Phosphorylated and total levels of AMPK, AS160, AKT and 4E-BP1, the level of phosphorylated ACC, and the level of atrogin-1 from vastus lateralis muscle lysates at serial time points after exercise were analyzed by Western blot. Actin is shown as a loading control. **b,** Absence of exercise-induced CaMK1 phosphorylation in muscle of WT and BCL2 AAA mice. Levels of CaMK1 phosphorylation in skeletal muscle lysates (thighs) from mice at rest (-) or after maximal exercise (+). Each lane represents lysates from a different mouse. CaMK1 phosphorylation was determined by Western blot analysis using an anti-p-CaMK1 (Thr177) antibody. Western blot analyses of total CaMK1 and actin are shown as controls.

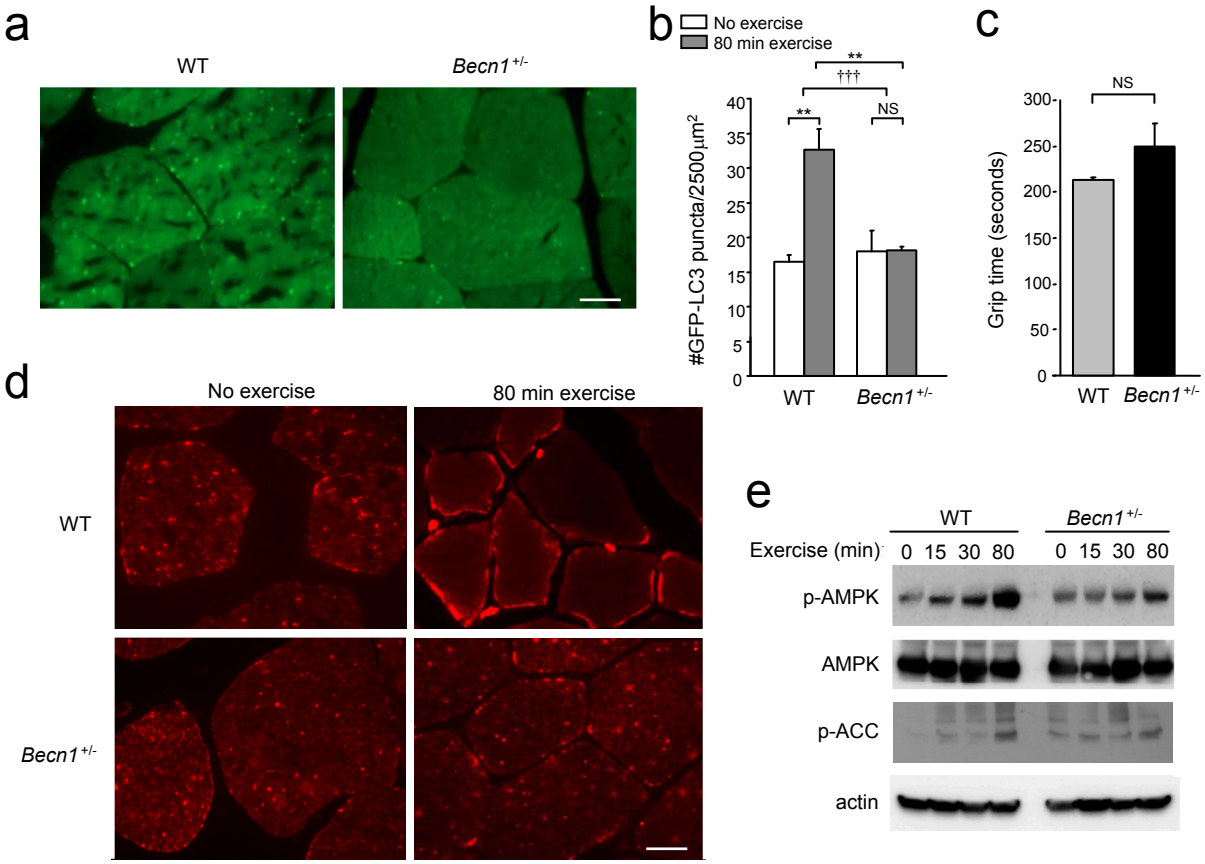

Supplementary Figure 14. Defects in exercise-induced skeletal muscle autophagy GLUT4 plasma membrane localization, and AMPK activation in *Becn1*$^{+/-}$ mice. a, Representative images of GFP-LC3 puncta (autophagosomes) in vastus lateralis muscle of GFP-LC3 *Becn1*$^{+/-}$ mice and GFP-LC3 WT littermates after a fixed duration (80 min) of exercise. **b,** Quantification of the GFP-LC3 puncta (autophagosomes) in the skeletal muscle of GFP-LC3 *Becn1*$^{+/-}$ mice and GFP-LC3 WT littermates in resting conditions (no exercise) and after a fixed duration and distance (80 min, ~900 m) of exercise (treadmill running). Results represent mean ± s.e.m. of 3 mice per experimental group. Muscles from *Becn1*$^{+/-}$ mice have significantly fewer mean GFP-LC3 puncta per area. **c,** Muscle strength of WT and *Becn1*$^{+/-}$ mice as measured by grip time on a wire mesh. Results represent mean ± s.e.m. of 6 mice per experimental group. **d,** Representative immunofluorescence images demonstrating subcellular localization pattern of GLUT4 in the skeletal muscle of *Becn1*$^{+/-}$ and WT littermates mice before and after 80 min of exercise. Similar results were observed in 3 mice per group. **e,** Western blot analysis of phosphorylated and total levels of AMPK and phosphorylated levels of ACC at indicated time points after exercise in the vastus lateralis muscle of *Becn1*$^{+/-}$ mice and WT littermates. Actin is shown as a loading control. For **a** and **d**, scale bar, 20 μm. $^{**}P < 0.01$, one-way ANOVA for comparison between groups; $^{\dagger\dagger\dagger}P < 0.001$, two-way ANOVA for comparison of magnitude of changes between different groups in mice of different genotypes. NS, not significant.

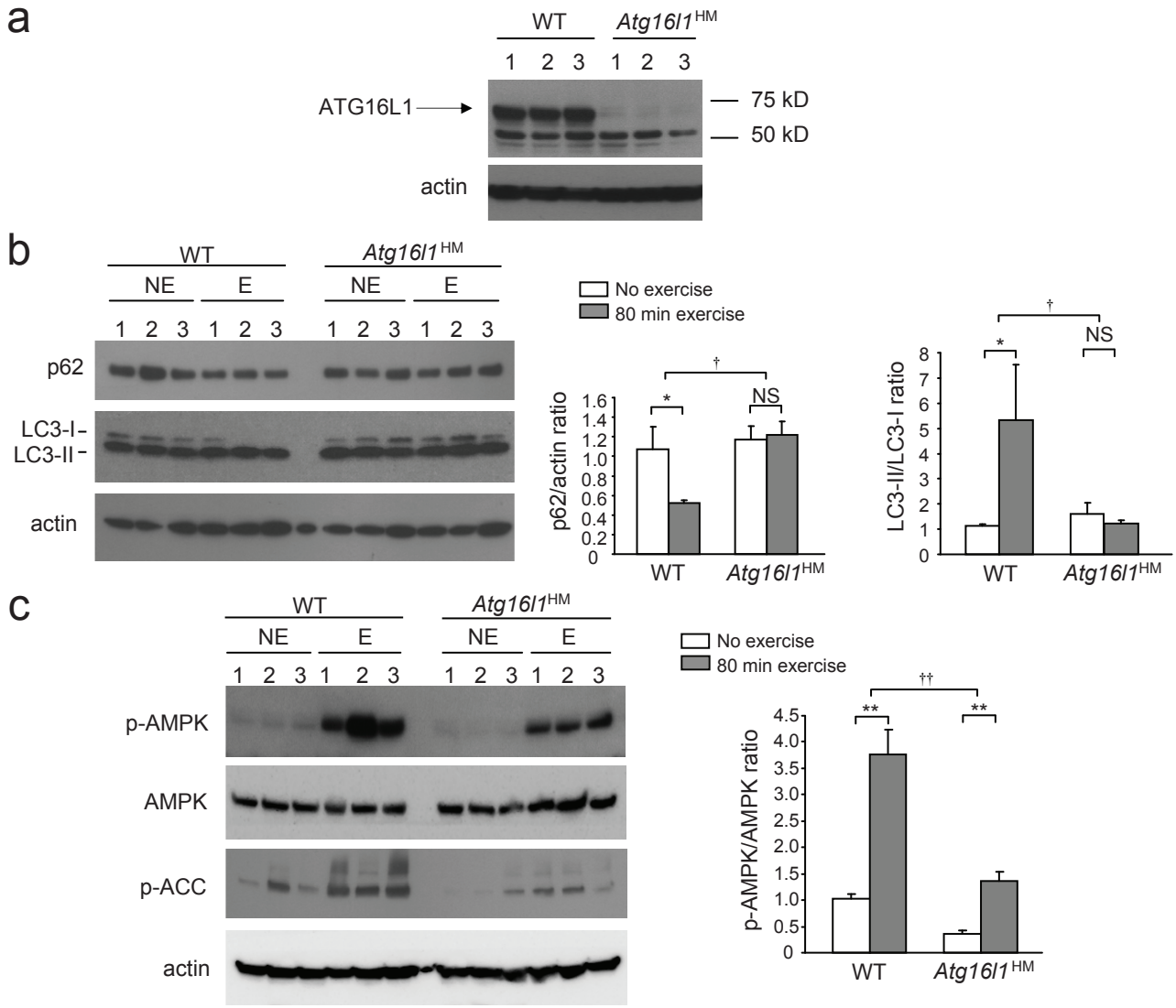

Supplementary Figure 15. *Atg16l1*^{HM} mice show defects in exercise-induced autophagy and AMPK activation in skeletal muscle. a, Western blot analysis of ATG16L1 expression in vastus lateralis muscles of WT and *Atg16l1*^{HM} mice. **b,** Western blot analysis of LC3 and p62 in vastus lateralis muscles of WT and *Atg16l1*^{HM} mice at resting conditions and after 80 min of exercise (left). Graphs showing quantification of p62/actin and LC3-II/LC3-I ratios at rest (NE) and after exercise (E) for 3 mice per group (right panels). Results represent mean ± s.e.m. **c,** Western blot analysis of phosphorylated and total levels of AMPK and phosphorylated levels of ACC in vastus lateralis muscles of WT and *Atg16l1*^{HM} mice at resting conditions and after 80 min of exercise (left). Graphs showing quantification of p-AMPK/AMPK ratios at rest (NE) and after exercise (E) (right). Results represent mean ± s.e.m. For **a-c**, actin is shown as a loading control. NE, no exercise; E, exercise. *$P < 0.05$, **$P < 0.01$, one-way ANOVA for comparison between groups; †$P < 0.05$, ††$P < 0.01$, two-way ANOVA for comparison of magnitude of changes between different groups in mice of different genotypes. NS, not significant.

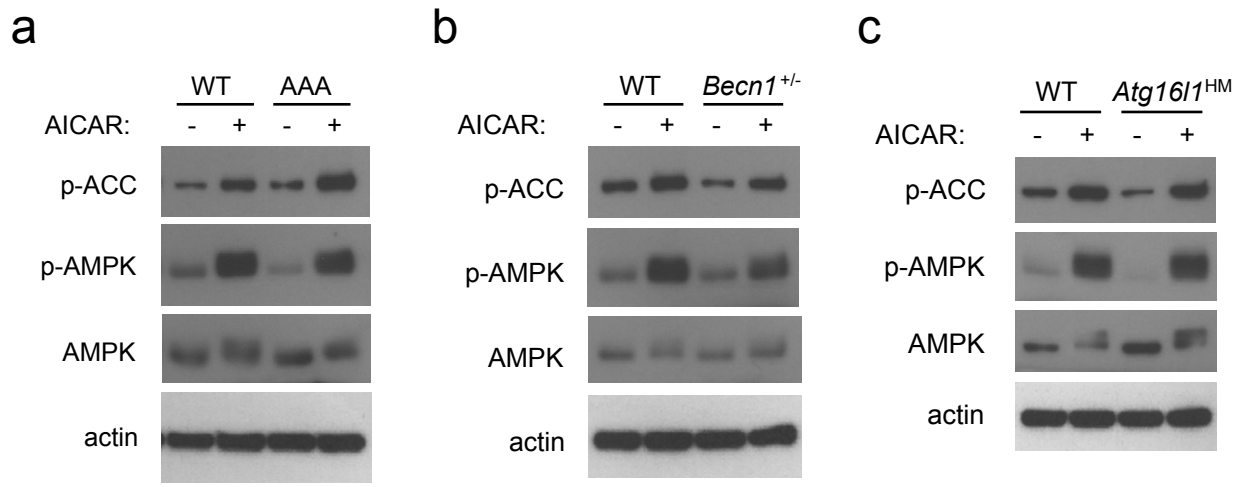

Supplementary Figure 16. Normal AICAR-induced AMPK activation in BCL2 AAA (a), *Becn1*$^{+/-}$ (b) and *Atg16l1*^{HM} (c) MEFs as compared to isogenic WT MEFs. Western blot analysis of phosphorylated and total levels of AMPK and phosphorylated ACC with or without AICAR treatment in indicated mutant and WT MEFs. Actin is shown as a loading control.

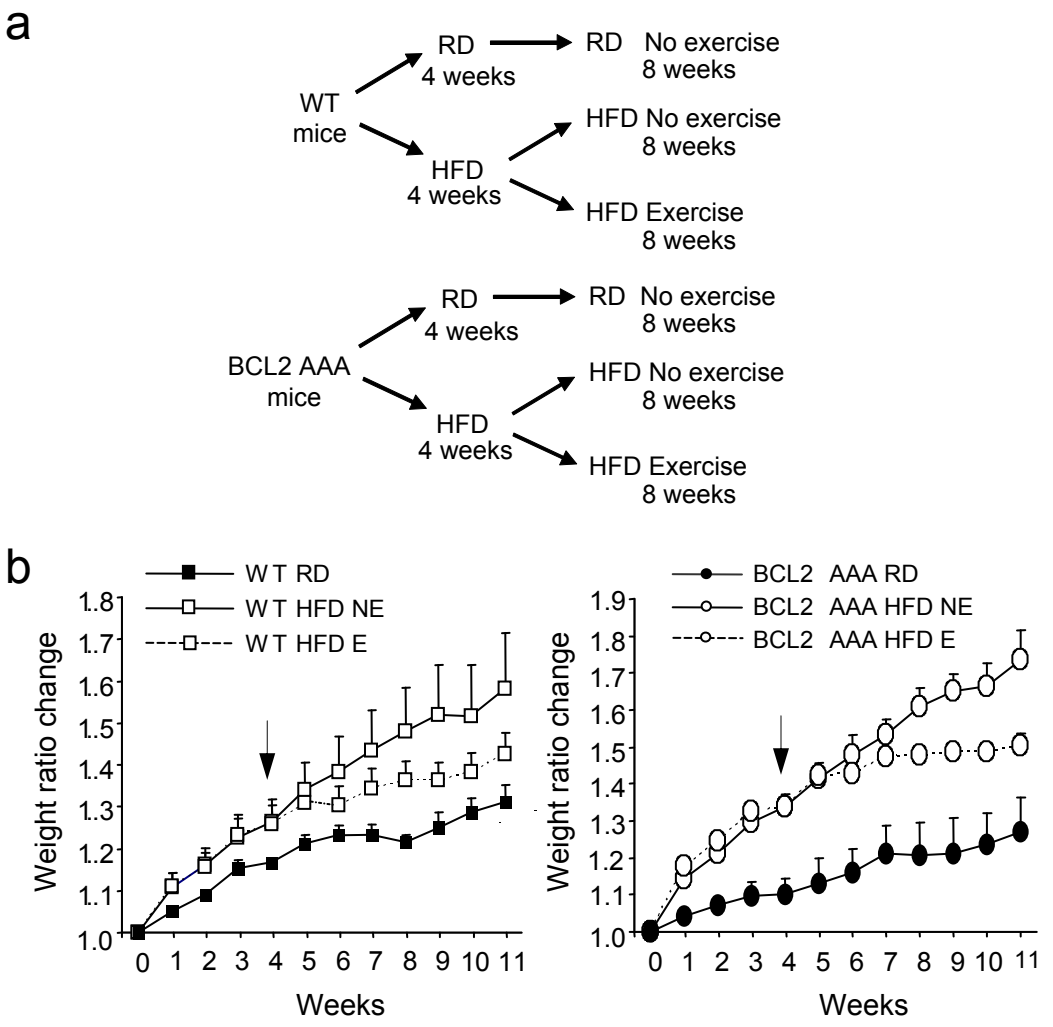

Supplementary Figure 17. Schematic representation of experimental design to study effects of exercise on high-fat diet (HFD)-induced insulin resistance and the effect of exercise on HFD-induced weight gain. a, WT and BCL2 AAA mice were randomized to receive regular diet (RD) or HFD for 4 weeks without exercise. The RD groups were maintained without exercise for an additional 8 weeks. At the end of 4 weeks, the HFD groups in each genotype were randomized to no daily exercise or a daily exercise regimen (see online Full Methods for details of regimen) for 8 weeks. **b,** Weight ratio changes during the time of HFD and exercise training. The arrow indicates the week of initiation of daily exercise. BCL2 AAA mice had increased weight gain during HFD treatment (p=0.043, one-way ANOVA) but daily exercise reduced weight gain similarly in BCL2 AAA and WT mice (p=NS, two-way ANOVA). NE, no exercise; E, exercise.

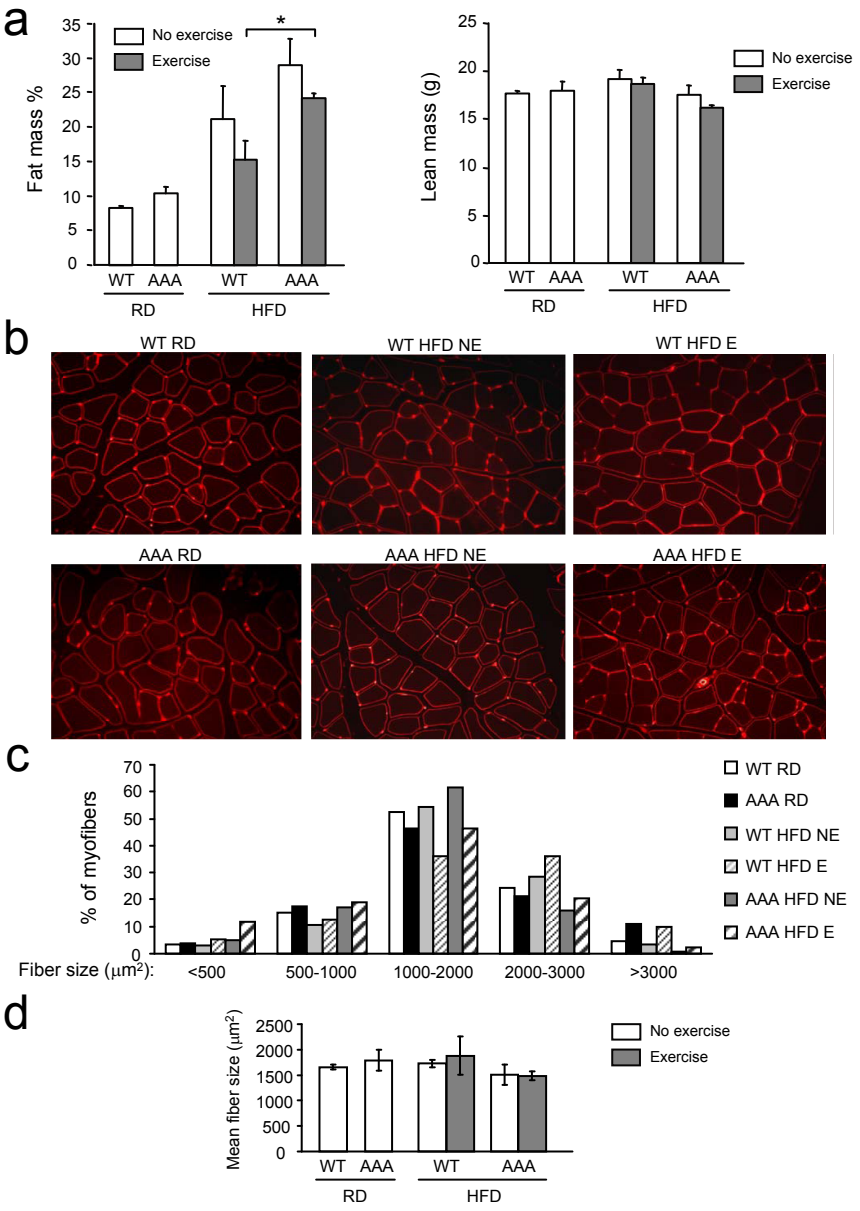

Supplementary Figure 18. Assessment of fat mass, lean mass, and muscle atrophy in WT and BCL2 AAA mice subjected to chronic HFD. a, Percentage of fat mass (left) and absolute weight of lean mass (right) as determined by NMR analysis at the end of the 12 weeks of HFD and 8 weeks of exercise training. Results represent mean ± s.e.m for 4-5 mice per experimental group. BCL2 AAA mice have increased fat mass compared to WT mice but no difference in lean mass. *$P < 0.05$ (one-way ANOVA). **b,** Representative images of thigh muscle cross-sections from WT or BCL2 AAA mice subjected to indicated condition stained with wheat agglutinin to outline each muscle fiber. **c,** Muscle fiber cross-sectional area in thigh muscles of WT or BCL2 AAA mice. Myofibers from three muscle cross-sections per mouse of three mice per genotype were measured. Approximately 200 myofibers were measured for each mouse. Results represent combined data for three mice per muscle group per genotype and are expressed as the percentage of myofibers within each category of cross-sectional area. **d,** Mean muscle fiber size of mice analyzed in **b-c**. Results represent mean ± s.d. for mean values of 3 mice per group. No differences were observed in muscle fiber cross-sectional area in **c** as measured by statistical analyses of fiber size density plots and no differences were detected in **d** for mean fiber size (one-way ANOVA).

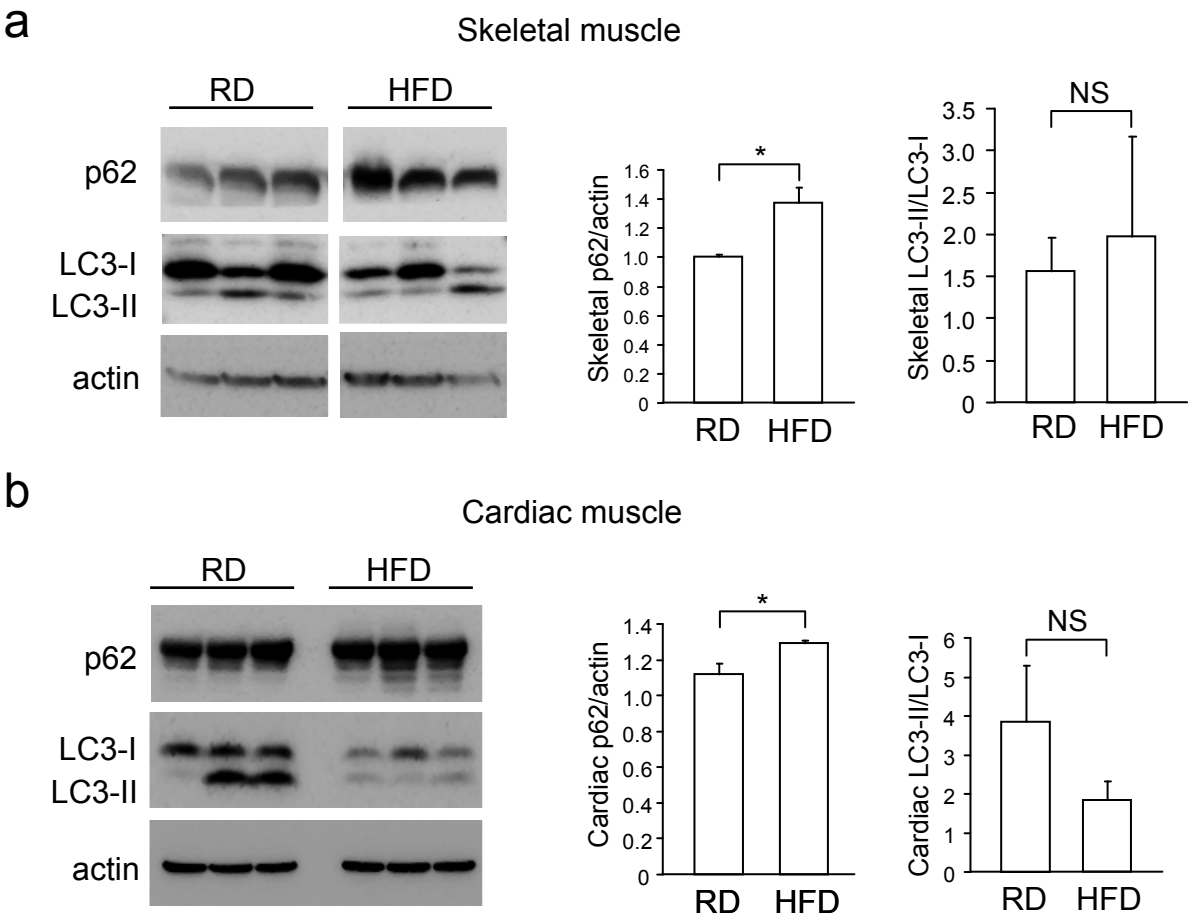

Supplementary Figure 19. Effect of high-fat diet (HFD) on baseline levels of autophagy in skeletal muscle (a) and cardiac muscle (b). Western blot analysis of p62 and LC3 in skeletal (vastus lateralis) and cardiac muscle lysates from mice that received 12 weeks of either regular diet (RD) or HFD. Three mice per experimental group are shown (left panels). Actin is shown as a loading control. Graphs showing quantification of p62/actin and LC3-II/LC3-I ratios during RD and HFD for 3 mice per group (right panels). Results represent mean ± s.e.m. *$P < 0.05$ (one-way ANOVA). NS, not significant.

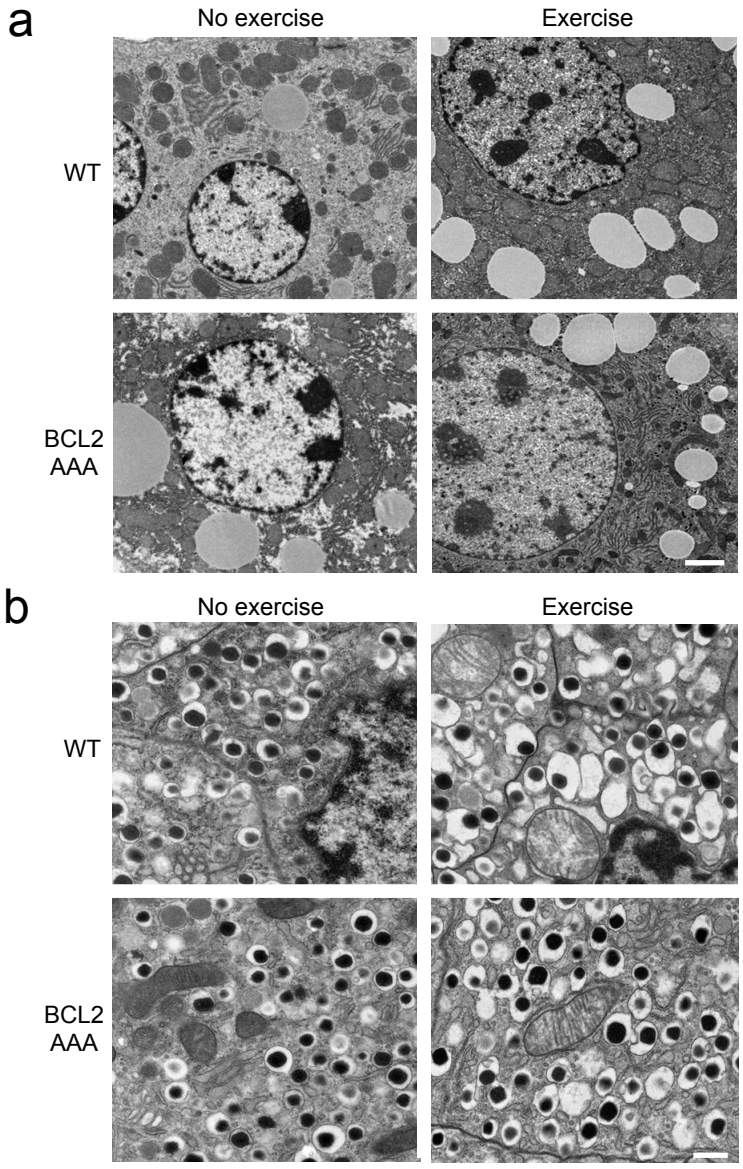

Supplementary Figure 20. Representative liver (a) or pancreatic β-cell (b) images of WT or BCL2 AAA mice analyzed by electron microscopy after 12 weeks of HFD with or without 8 weeks of exercise training. No apparent differences were observed between any of the groups shown. More lipid droplets were observed in the hepatocytes of HFD-fed versus RD-fed animals (images not shown for RD-fed animals). In both the livers and pancreas of BCL2 AAA mice, ultratructural findings associated with tissue-specific knockout of autophagy genes (e.g. *Atg5* or *Atg7*), such as the accumulation of damaged mitochondria; swollen or dilated ER; or vacuolar changes, apoptosis or diminished β-cell mass were not observed. Shown in (**a**) are representative images of typical hepatocytes that contain a variable number of lipid droplets. Shown in (**b**) are representative images of typical β-cells that contain normal appearing insulin granules (dense central core surrounded by electron lucent area). No ultrastructural abnormalities were detected in the exocrine pancreas of any group (data not shown). Scale bar, **a,** 2 μm and **b,** 0.5 μm.

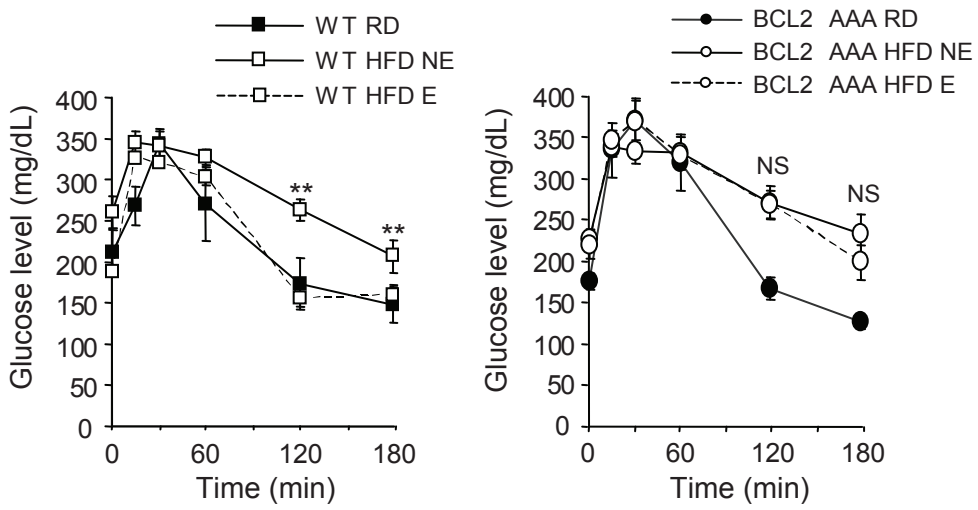

Supplementary Figure 21. Five weeks of exercise training protects WT, but not BCL2 AAA, mice from HFD-induced glucose intolerance. Oral glucose tolerance test (OGTT) after 9 weeks of HFD with 5 weeks of exercise training.

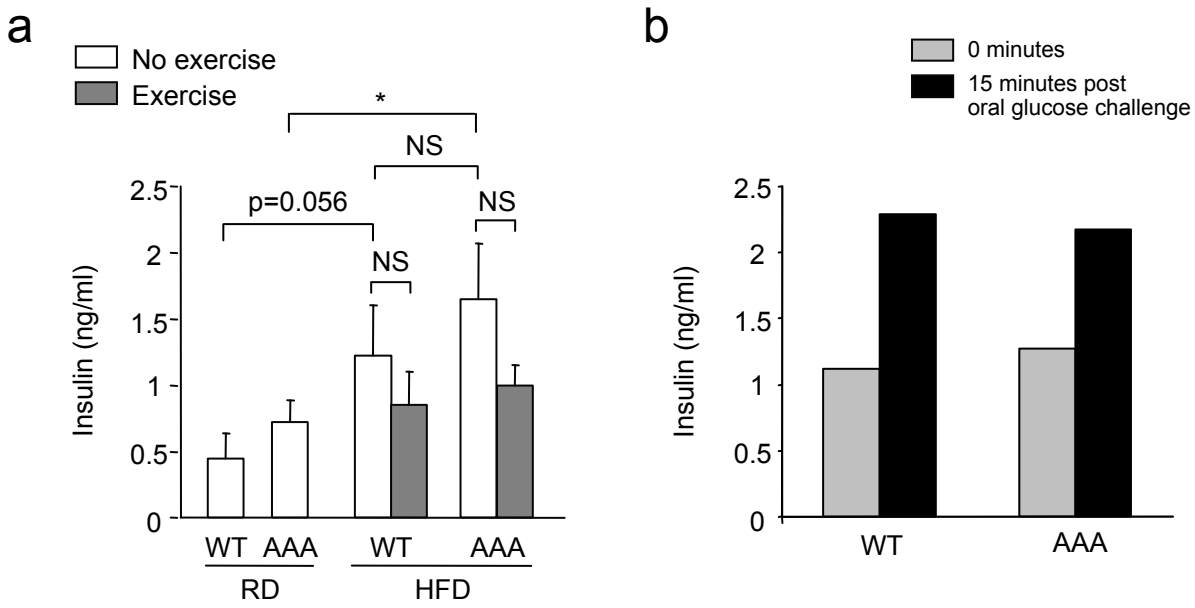

Supplementary Figure 22. Insulin levels are similar in HFD-fed WT and BCL2 AAA mice during fasting conditions and in response to oral glucose challenge. a, Plasma insulin levels at the end of the 12 weeks of HFD and 8 weeks of exercise training in mice after an overnight fast. Results represent mean ± s.e.m for 4-5 mice per experimental group. *$P < 0.05$ (one-way ANOVA). NS, not significant. **b,** Plasma insulin levels at the end of 12 weeks of HFD at 0 and 15 min after oral glucose challenge. Results represent values from pooled plasma from 5 mice per experimental group. No significant differences were observed between WT and BCL2 AAA mice (ANOVA).

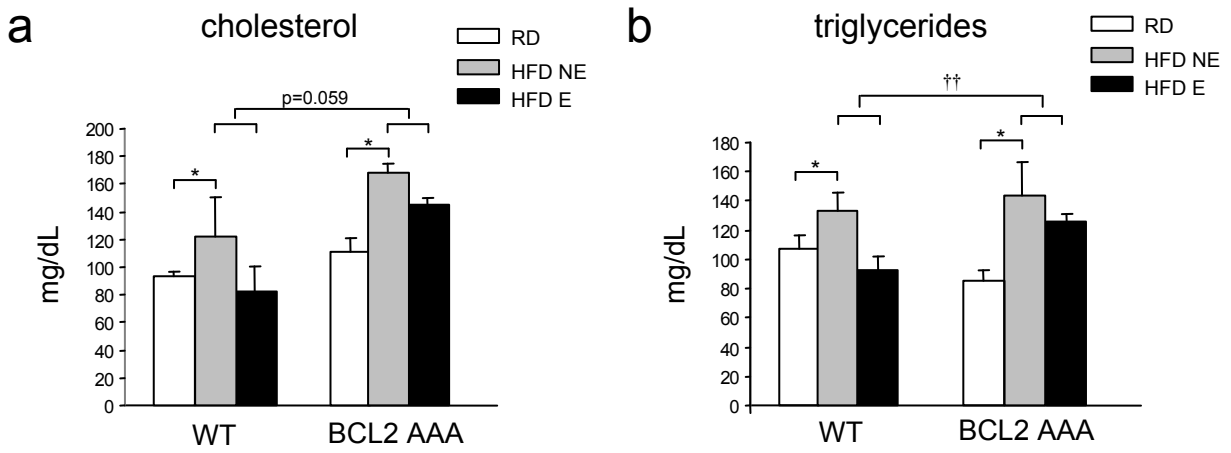

Supplementary Figure 23. Serum cholesterol (a) and triglcyeride (b) levels of WT and BCL2 AAA mice after 12 weeks of HFD and 8 weeks of exercise training. Results represent mean ± s.e.m. for 4 mice per experimental group. Serum triglycerides and cholesterol increased in both HFD-fed WT and BCL2 AAA mice. Values returned to baseline with exercise in WT but not in BCL2 AAA mice. **P* < 0.05, one-way ANOVA for comparison between groups; ††*P* < 0.01, two-way ANOVA for comparison of magnitude of changes between different groups in mice of different genotypes.

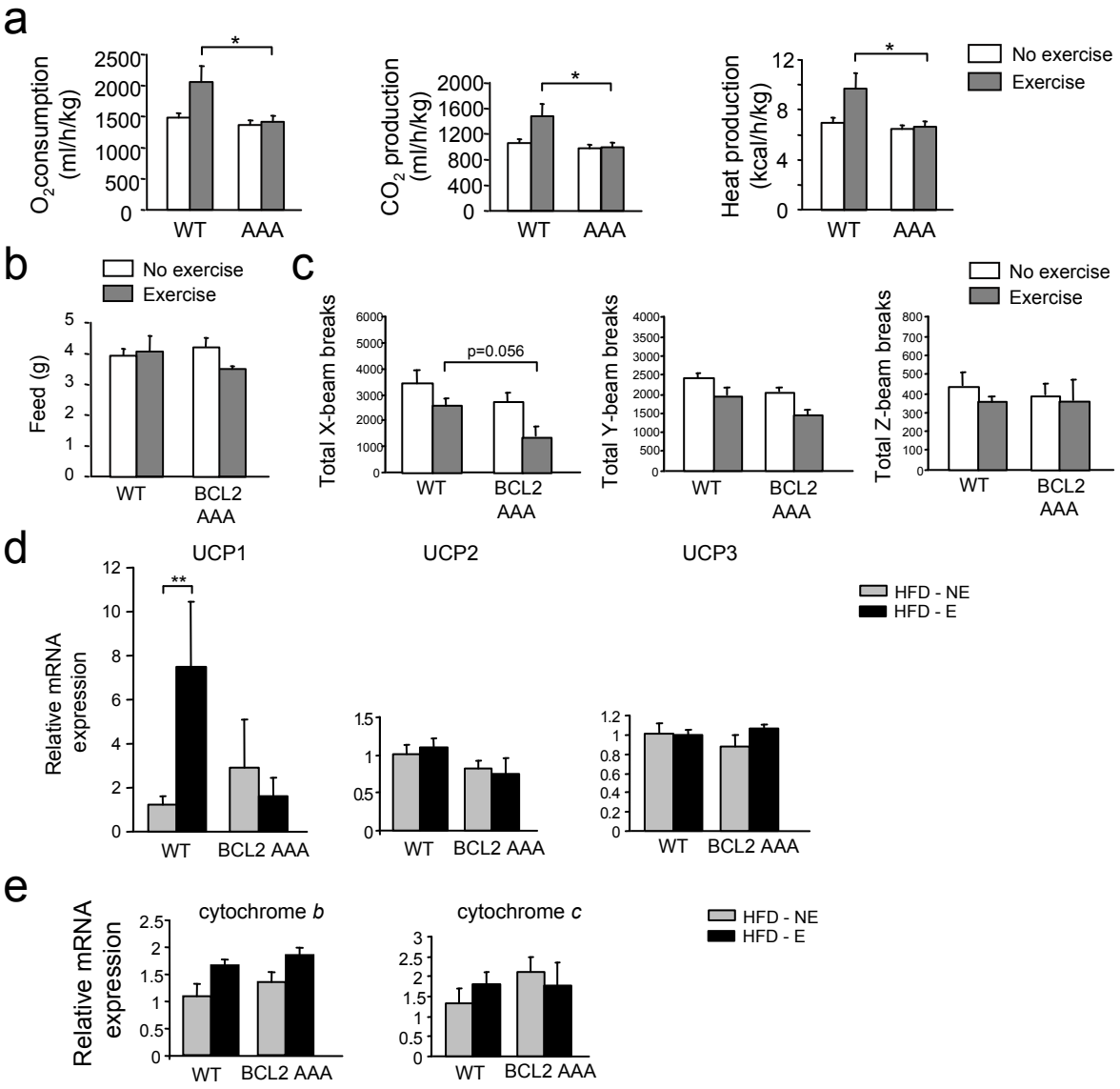

Supplementary Figure 24. Metabolic activity, food intake, physical activity and mitochondrial markers in HFD-fed WT and BCL2 AAA mice with and without exercise training. a, Effects of exercise training on metabolic activity of WT and BCL2 AAA mice. Oxygen consumption, carbon dioxide production and heat production rates were measured over the 12 h dark period. **b,** Daily food intake over the 12 h dark period at the end of 12 weeks of HFD and 8 weeks of exercise training. **c,** Three-dimensional movement activity of WT and BCL2 AAA mice over a four day period at the end of the 12 weeks of HFD and 8 weeks of exercise training. For **a-c**, results represent mean ± s.e.m. for 4-5 mice per experimental group. For **b-c**, no significant differences were observed between groups (ANOVA) with the exception of a trend towards decreased activity in the x-axis for HFD-fed, exercised BCL2 AAA mice compared to WT mice ($p = 0.056$, ANOVA). *$P < 0.05$ (Wilcoxon rank test). **d-e,** Real-time PCR analysis of relative levels of mRNA expression for UCP1, UCP2, and UCP3 (**d**) and for cytochrome *b* and cytochrome *c* (**e**) in vastus lateralis muscle of WT and BCL2 AAA mice at the end of HFD treatment and 8 weeks of exercise training. For **d-e**, results represent mean ± s.e.m. for 4 mice per experimental group, and the only significant difference was an increase in UCP1 expression in the exercise compared to no exercise groups in WT mice (**$P < 0.01$, ANOVA).